PHOTO PHYSICAL PROPERTIES OF CAFFEINE AND CU (II)-CAFFEINE COMPLEX

A thesis submitted to the School of Graduate Studies

Addis Ababa University

In partial Fulfillment of the Requirements for the

Degree of Master of Science in Physics

By Tesfay G/medhin

Addis Ababa, Ethiopia

September 2007

ADDIS ABABA UNIVERSITY
FACULTY OF SCIENCE
DEPARTMENT OF PHYSICS

The undersigned here by certify that they have read and recommended to the Faculty of Science School of Graduate Studies for acceptance a thesis entitled “photo physical properties of caffeine and Cu (II)-Caffeine complex” by Tesfay G/medhin in partial fulfillment of the requirements for the degree of Master of Science in Physics.

Name	Signature
Dr. Araya Asfaw, Advisor	————————
Dr. Mesfine Redi, Co-Advisor	————————
Dr. S.K.Ghoshal, Examiner	————————
Dr. Yonas Chebude, Examiner	————————

To family

TABLE OF CONTENTS

Abstract

In this thesis UV/Vis absorption spectra of caffeine in water and dichloromethane, copper sulphate, and mixture of caffeine and copper sulphate in water solution is investigated. UV/Vis absorption spectrum of Cu (II)-Caffeine complex is also investigated as a function of time during refluxing to check complex formation. The molar decadic absorption coefficient of caffeine is calculated. Fluorescence emission spectra of Cu (II)-Caffeine complex is also investigated and compared with its absorption band. Area normalization analysis method is used. Finally, a better derivative fluorescence method for determination of caffeine content of substances is recommended.

Key words: Absorbance, Molar decadic absorption coefficient, Reflux, Complex formation, Derivative Fluorescence, Is-emission point, Area normalization

Chapter One

1. Introduction

Coffee is an evergreen tropical shrub belonging to rubiaseae family, which comprises at least 66 species of the genus coffee [1]. Its size, color and the color of its flowers differ from species to species [1, 2, 3].

Coffee Arabica, which is highly demanded in world market, is one of the coffee species found in our country. It grows in fertile, slightly acidic soil [4], average annual temperature between 288.15 K and 298.15 K, altitude 1200 m-1500 m, and average rainfall of 1100 -1500 mm [5].

It is the most agricultural commodity ranks second to petroleum interims of the dollar treaded worldwide and worth up to $14 billion annually [1, 2]. More than 80 countries export it as raw, roasted, grinded or soluble products to more than 165 countries in the world [6]. Arabica accounts for two third and Robusta one third of world's production.

Coffee is a big deal in Ethiopia as it is enjoyed everywhere in the planet [7]. It is not only used as a stimulant but also enjoyed by special ceremonies it has in special circumstances such as birth, marriage, holidays and some other occasions. The lives of many farmers and the economy of our country highly depend up on this exotic plant. It contributes 60% of foreign exchange, which is a very large figure compared to other products and services [5, 8].

The main composition of coffee are; Ash and Minerals, free amino acids, proteins, carbohydrates, polysaccharides lipids, acids, volatile compounds, and caffeine. Water-soluble components are aroma (0.1%), lipids (0.2%), lipids (0.3%), organic acid (0.5%), caffeine (1%), water (2%), minerals (3%), chlorogenic acid (4%), polysaccharides (6%), and phenol polymers (8%) [9-14]. of these compounds, caffeine is believed to be the component responsible for stimulating effects [12, 15].

Caffeine (1, 3, 7-trimethylxanthine) is naturally occurring substance found in the leaves, seeds and fruits of at least 63 plant species [18]. Coffee, cocoa beans, kola nuts, chocolate, and tealeaves are the most common sources. It is a plant-derived alkaloid;

white silky, odorless compound, which melts at 236 °C and sublimes at around 178 °C. It has got a structure shown below with chemical formula, $C_8H_{10}N_4O_2$

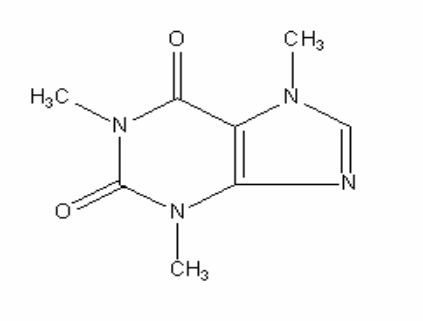

Fig. 1: Caffeine structure

Average cup of coffee or tea in the United States is reported to contain between 40 and 150 mg caffeine [15], although specialty coffees may contain much higher doses [16]. Caffeine undergoes rapid absorption following oral administration. A single 130 mg oral dose in 36 subjects produced peak plasma concentrations of 2.5-6.8 mg/l (mean 4.0 mg/L) within 20-40 minute [17]. Approximately 90% of the caffeine in a cup of coffee is absorbed from the stomach within 20 min with peak plasma concentrations occurring approximately 40-60 min later. The drug is widely distributed and can undergo placental transfer, which is the reason for limiting dietary intake of caffeine during pregnancy. More than 25 metabolites of Caffeine have been identified and many are pharmacologically active. During elimination, approximately 85% of a dose is excreted in the urine within 48 h, with approximately 1% as unchanged drug. Although the plasma half-life is reported to be 2-10 h (mean 4 h) in adults, it maybe as long as 4 days in neonates due to impaired metabolism [13].

This chemical has identified positive and negative physiological effects. It stimulates the central nervous systems at higher levels, the cortex, medulla and the spinal cord at higher doses [12, 19]. Mild cortex stimulation appears to be beneficial resulting in more thinking and less fatigue. It improves attention or concentration [14]. It is considered that caffeine provides a potential possibility to regulate the biological activity of aromatic dyes and antibiotics, which is of particularly importance for chemical applications [20].

Intensive research has been conducted studding the effects of vasoactive substances on peripheral blood pressure. Caffeine has been examined thoroughly concerning its role on blood pressure and cardiovascular risk [21]. But the opposite effect has been absorbed [22]. Another research is conducted to alleviate this controversy and found neither regular nor decaffeinated coffee affects significantly peripheral systolic pressure. Numerous factors and mechanisms are involved in the discrepancies absorbed at the results of various studies. The difference in sensitivity between normative and hypertensive subjects. Age is another factored that may be involved in the extent of the caffeine effect on peripheral systolic pressure. It has been found that it is increased more in older than younger subjects after caffeine consumption [23]. Other factors such as mental and behavioral stress play a negative role in caffeine effects of blood pressure [24].

It can be profoundly toxic, resulting in arrhythmia, tachycardia, vomiting, convulsions, coma and death. More than 10 gm are needed for such toxicity to occur in man [24]. Fatal caffeine overdose is relatively uncommon. However, it is report two cases: one, which may have resulted from misidentification of the drug and another that appears to involve misuse of a dietary supplement. In both cases, the cause of death was attributed to caffeine intoxication and the manner of death was accident [25].

Concern over to possible toxic effects and undesirable physiological effects of caffeine have lead to an increasing demand for decaffeinated green beans [15]. Decaffeination was first practiced in 1905 in Germany [3]. There are different decaffeination-techniques; water decaffeination, solvent decaffeination and carbon dioxide decaffeination are the most widely used. Due to the additional labor equipments involved these decaffeinated coffee are expensive even thought they are known to lose much of their flavor during processing.

Scientists in Japan able to produce transgenic plant with 70% reduced caffeine [5]. However, using genetically engineered plant is a controversial, which the altered genes could be handed on to other species and may also affect human health [22].

By breeding 3000 Ethiopian coffee plants, scientists from Brazil found bushes all derived from the same plant were virtually caffeine free containing 15 times less stimulant than commercial strains [5, 22]. This discovery hopefully eliminates the labor

and cost of decaffeination process and the loss of natural flavor and aromas of coffee. Identifying these coffee species, which does have very low caffeine, enables our country and coffee farmers benefited much from it since 8-10 present of the world export market is demanding decaffeinated coffee [27].

Many analytical methods have been developed for qualitative and quantitative analysis of caffeine such as UV/Vis and IR absorption [28, 9], amprometric titration volumetric analysis, various chromatographic and solid-phase microextractions, and other combined methods. However, the perspiration was usually involved in these methods. In order to avoid fussy separation procedures, some researchers used mathematical processing [10, 28] to determine caffeine by UV/Vis spectrometry. And others use IR to illuminate the interference [28]. Although these methods could improve selectivity, meanwhile, it caused the reduction of sensitivity. The great interest in fluorescence of caffeine is mainly to develop a simple and accurate method for the determination of caffeine from coffee and other substances in water solution.

Previous thesis works [9, 18] practiced fluorescence quenching method of determining caffeine from coffee beans. In this work absorption and fluorescence properties of caffeine complexes formed with copper metal-ion are studied for possible analytical applications.

Chapter two

2. Electromagnetic Radiation and Its Interaction with Matter

2.1 The Macroscopic Maxwell Equations

All macroscopic aspects of the static and dynamics of electromagnetic field in the presence of material media are described by Maxwell's equations [27]. These equations are the most fundamental description of electric and magnetic field [28]. Differential form of these axioms in the international system of units (SI) given by

$$\vec{\nabla} \cdot \vec{D} = \rho \tag{2.1}$$

$$\vec{\nabla} \cdot \vec{B} = 0 \tag{2.2}$$

$$\vec{\nabla} \times \vec{E} = -\frac{\partial \vec{B}}{\partial t} \tag{2.3}$$

$$\vec{\nabla} \times \vec{H} = \frac{\partial \vec{D}}{\partial t} + \vec{J}\,. \tag{2.4}$$

For a given position vector $\vec{r}$ (m) and time t(s) Maxwell's equations couple electric displacement vector $\vec{D}$ (C/m^2) and charge density ρ (C/m^3), magnetic induction $\vec{B}$ (T) and electric field strength $\vec{E}$ (V/m), magnetic field strength $\vec{H}$ (A/m) and total electric current density $\vec{J}$ (A/m^2).

When an electric field applied to dielectric medium composed of polarizable molecule, it acquires an average dipole moment $\vec{p}$ proportional to the local electric field $\vec{E}$ [26]. If there are N such molecules per unit volume the macroscopic polarization $\vec{P}$ is given by

$$\vec{P} = N\vec{p} = \chi_e \varepsilon_0 \vec{E} \tag{2.5}$$

where ε_0 permittivity in vacuum, χ_e electric susceptibility and $\vec{P}$ electric dipole moment per volume. Material media response is expressed as

$$\vec{D} = \varepsilon_0 \vec{E} + \vec{P} \tag{2.6}$$

$$\vec{B} = \mu_0 \vec{H} + \mu_0 \vec{M} \, . \tag{2.7}$$

Using equation (2.5) for $\vec{P}$, the electric displacement will be

$$\vec{D} = \varepsilon_0 \vec{E} + \chi_e \varepsilon_0 \vec{E} \tag{2.8}$$

$$\vec{D} = \varepsilon_0 \vec{E}(1 + \chi_e) \tag{2.9}$$

Where $1 + \chi_e = \varepsilon_r$.

Since $\varepsilon = \varepsilon_r \varepsilon_0$ equation (2.6) can be written

$$\vec{D} = \varepsilon \vec{E} \, . \tag{2.10}$$

Similarly in the presence of magnetic materials, the applied magnetic field induces a density $\vec{J}$ of magnetization current and hence a magnetization $\vec{M}$ in the materials [26]. Therefore $\vec{B}$ becomes

$$\vec{B} = \mu_0 \vec{H} + \vec{M} \tag{2.11}$$

Where $\vec{M} = \mu_0 \chi_m \vec{H}$. Using this equation (2.11) becomes

$$\vec{B} = \mu_0 \vec{H}(1 + \chi_m) \tag{2.12}$$

With $\mu_r = 1 + \chi_m$ and $\mu = \mu_0 \mu_r$. equation (2.12) can be rewritten as

$$\vec{B} = \mu\vec{H} \tag{2.13}$$

where $\vec{M}$ is magnetization vector (magnetic dipole moment per unit volume induced by magnetic field) μ_0 permeability in vacuum and μ_r is the relative permeability,

2.2 Electromagnetic Wave

The energy of a photon is transported in the form of electromagnetic wave. The equations of electromagnetic wave result from Maxwell's equations [25, 26]. From equation (2.3) we have

$$\vec{\nabla} \times \vec{E} = -\frac{\partial \vec{B}}{\partial t}. \tag{2.14}$$

Applying the curl operation to both sides of equation (2.14)

$$\vec{\nabla} \times \vec{\nabla} \times \vec{E} = -\nabla \times \frac{\partial \vec{B}}{\partial t} = -\frac{\partial}{\partial t}(\vec{\nabla} \times \vec{B}). \tag{2.15}$$

Using the general identity of vector calculus $\vec{\nabla} \times \vec{\nabla} \times \vec{E} = \vec{\nabla}(\vec{\nabla} \cdot \vec{E}) - \nabla^2 \vec{E}$ and by substituting to the left hand side of equation (2.15)

$$\vec{\nabla}(\vec{\nabla} \cdot \vec{E}) - \nabla^2 \vec{E} = -\frac{\partial}{\partial t}(\vec{\nabla} \times \vec{B}). \tag{2.16}$$

Again, for $\vec{B} = \mu_0 \vec{H}$ and ρ =0 (2.4) becomes

$$\vec{\nabla} \times \frac{\vec{B}}{\mu_0} = \frac{\partial \vec{D}}{\partial t}. \tag{2.17}$$

Substituting the right hand side of equation (2.17) in to equation (2.16)

$$\vec{\nabla}(\vec{\nabla}\cdot\vec{E})-\nabla^2\vec{E}=-\frac{\partial}{\partial t}\mu_0\frac{\partial\vec{D}}{\partial t}. \tag{2.18}$$

Since for optically linear and isotropic medium $\vec{\nabla}\cdot\vec{E}=0$, equation (2.18) becomes

$$\nabla^2\vec{E}=\mu_0\frac{\partial^2\vec{D}}{\partial t^2}. \tag{2.19}$$

If we substitute equation (2.6) for $\vec{D}$ then equation (2.19) will be

$$\nabla^2 E=\mu_0\frac{\partial^2}{\partial t^2}(\varepsilon_0\vec{E}+\vec{P}) \tag{2.20}$$

$$\nabla^2\vec{E}-\mu_0\varepsilon_0\frac{\partial^2\vec{E}}{\partial t^2}=\mu_0\frac{\partial^2\vec{P}}{\partial t^2}. \tag{2.21}$$

The above equation is wave equation for dielectric medium with no free charges. In vacuum or free space the polarization is zero ($\vec{P}$ =0), so equation (2.21) can be reduced to

$$\nabla^2\vec{E}-\mu_0\varepsilon_0\frac{\partial^2\vec{E}}{\partial t^2}=0. \tag{2.22}$$

Since $\vec{J}=0$ similarly for magnetic field by using equation (2.4) and applying the curl operator to both sides the equation it becomes

$$\vec{\nabla}\times\vec{\nabla}\times\vec{H}=\vec{\nabla}\times\frac{\partial\vec{D}}{\partial t}. \tag{2.23}$$

Using the general identity equation (2.23) becomes

$$\vec{\nabla}(\vec{\nabla}\cdot\frac{\vec{B}}{\mu_0})-\nabla^2\vec{B}/\mu_0=\varepsilon_0\frac{\partial}{\partial t}(\vec{\nabla}\times\vec{E})\,. \tag{2.24}$$

Since $\vec{\nabla}\cdot\vec{B}=0$ equation (2.24) becomes

$$\nabla^2\vec{B}=\mu_0\varepsilon_0\frac{\partial^2\vec{B}}{\partial t^2} \tag{2.25}$$

$$\nabla^2\vec{B}-\mu_0\varepsilon_0\frac{\partial^2\vec{B}}{\partial t^2}=0\,. \tag{2.26}$$

Equation (2.22) and (2.26) are the wave equations for electromagnetic field in vacuum. They are the simplest, indeed the only equations having a solution undamped vector waves traveling in three dimensions at any frequency and constant velocity [26]. Using separation of variables the solution of equation (2.22) and (2.26) will be

$$\vec{E}(\vec{r},t)=\vec{\varepsilon}E_0\exp-i(\omega t-kz) \tag{2.27}$$

$$\vec{B}(\vec{r},t)=\vec{\varepsilon}B_0\exp-i(\omega t-kz) \tag{2.28}$$

where k is magnitude of wave vector. Since electric and magnetic fields are real, observable quantities [26], for electromagnetic wave moving along positive z direction equation (2.27) and (2.28) become

$$\vec{E}(\vec{z},t)=E_0\cos(\omega t-kz+\delta) \tag{2.29}$$

$$\vec{B}(\vec{z},t)=B_0\cos(\omega t-kz+\delta) \tag{2.30}$$

where δ is phase shift.

Equation (2.21) is a wave equation for propagation in a material media. In this case for a wave propagating in +z direction in a weakly absorbing medium possible solution is [28].

$$\vec{E}(z,t) = \vec{\varepsilon} E_0 \exp(-\alpha z)\cos(\omega t - kz) \tag{2.31}$$

where α is the natural absorption coefficient and $k = 2\pi n/\lambda$ is the magnitude of wave vector. Both α and k are related to imaginary and real parts of the linear susceptibility $\chi^{(1)}(-\omega;\omega)$, and to the refractive index n and the speed of light in the medium by the following equations

$$\alpha = \frac{\omega}{c}\,\mathrm{Im}\left\{\chi^{(1)}(-\omega;\omega)\right\} \tag{2.32}$$

$$n = \sqrt{1 + R_e\left\{\chi^{(1)}(-\omega;\omega)\right\}} \tag{2.33}$$

$$k = \frac{\omega}{c} = \frac{n\omega}{c_0} = \frac{2\pi n}{\lambda_0}.$$

Here, $c_0 = 2.9979 \cdot 10^8\ \mathrm{m\,s^{-1}}$ is the speed of light in vacuum and λ_0 is wavelength of light in vacuum. For non-absorbing medium or far from the resonance $\chi^{(1)}$ is a real quantity and related to a property n, which is commonly known as the refractive index of the material.

The real and imaginary parts of susceptibility are in certain cases coupled through Kramers-Kronig relations such as

$$R_e\left\{\chi^{(1)}(\omega_{eg})\right\} = \frac{2}{\pi}\int_0^\infty \frac{\omega\,\mathrm{Im}\,\chi^{(1)}(-\omega;\omega)}{\omega_{eg}^2 - \omega^2}\,d\omega \tag{2.34}$$

where ω_{eg} is the frequency of maximum absorption. The equation holds for $\chi^{(1)}(-\omega;\omega)$ and thus relates the absorption coefficient (imaginary part) to the refractive index (real part) of the medium. For a static field the frequency is zero ($\omega = 0$) the susceptibility is expressed as $\chi^{(1)}(0;0)$. $\chi^{(1)}(0;0)$ is related to the relative permittivity or dielectric constant of the medium ε_r

$$\chi^{(1)}(0;0) = \varepsilon_r - 1. \tag{2.35}$$

2.3 Time Dependent Perturbation Theory

If a system has initially a wave function ψ_i and energy E_i and the final state ψ_f and E_f the new Hamiltonian $\hat{H}$ due to perturbation is the sum of unperturbed $\hat{H}^{(0)}$ and the perturbing $H^{(1)}$ Hamiltonians [26, 31]. Therefore

$$\hat{H} = \hat{H}^{(0)} + \hat{H}^{(1)}. \tag{2.36}$$

If the perturbation is due to an electric field the change in Hamiltonian due to this field can be

$$\hat{H}^{(1)} = \hat{\vec{\mu}} \cdot \vec{E} \tag{2.37}$$

where $\hat{\vec{\mu}}$ and $\vec{E}$ represent dipole operator and electric field respectively. Rate of transition probability of the system dP_{fi}/dt is expressed through the Fermi Golden rule [26] as

$$\frac{dP_{fi}}{dt} = \frac{1}{6\varepsilon_0 \hbar^2} \left|\mu_{fi}\right|^2 \rho(\nu_{fi}). \tag{2.38}$$

The rate of transition depends on transition dipole moment and energy density of radiation. It is also expressed in terms of Einstein's coefficient of induced absorption (B_{fi}) [26]. Hence

$$\frac{dp_{fi}}{dt} = B_{fi}\rho(\nu_{fi}) \tag{2.39}$$

where B_{fi} is the Einstein's coefficient for the induced absorption and is expressed as

$$B_{fi} = \frac{1}{6\varepsilon_0 \hbar^2} \left| \mu_{fi} \right|^2 . \tag{2.40}$$

2.4 Comparison of Rate Probability with Experimental Quantities

Now we relate rate of probability (microscopic molecule) to molar decadic absorption coefficient (macroscopic). Since the square of electric field is directly proportional to intensity of the light [27], using equation (2.31).

$$I(z) \propto \left\langle \left(E(z,t)\right)^2 \right\rangle_T \tag{2.41}$$

$$I(z) \propto \left\langle \left(E_0 \exp(-\alpha z)\cos(\omega t - Kz)\right)^2 \right\rangle_T \tag{2.42}$$

$$\propto E_0{}^2 e^{-\alpha z} . \tag{2.43}$$

This implies that

$$I(z) = I_0 e^{-\alpha z} \tag{2.44}$$

But absorption coefficient α related to molar absorption coefficient κ and molar decadic absorption coefficient $\varepsilon(\tilde{\nu})$ [29, 31] as follow.

$$\alpha = \kappa c \tag{2.45}$$

$$\alpha = \ln(10)\varepsilon(\tilde{\nu})c . \tag{2.46}$$

So equation (2.44) can be rewrite in terms of equation (2.45) and (2.46) as (when *z*=l)

$$I(z,\tilde{\nu}) = I_0 e^{-\kappa c l} = I_0 e^{-\ln(10)\varepsilon(\tilde{\nu})cl} . \tag{2.47}$$

For very diluted and short path length the above equation becomes

$$I = I_0(1 - \varepsilon c l \ln(10)) . \tag{2.48}$$

Differentiate both sides of equation (2.48) we have

$$-dI = I_0 \varepsilon c \ln(10) dl . \tag{2.49}$$

We can also express c as follow

$$c = \frac{N}{N_a} \tag{2.50}$$

where N is number of molecules and N_a Avogadro numbers, therefore equation (2.49) becomes

$$-dI = \varepsilon \frac{N}{N_a} I_0 \ln(10) dl . \tag{2.51}$$

dP/dt is the rate of probability for a single molecule changes as a result of absorption of radiation under perturbing effect of electric field of radiation then $P_{fi} N\mathrm{d}l$ is the number of molecules excited in a layer dl with an energy absorption $h\nu_{fi}$ So the loss in intensity can be written as follow [30, 31].

$$-dI = \frac{dP_{fi}}{dt} N h\nu_{fi} dl . \tag{2.52}$$

Comparing equation (2.51) an experimental quantities with equation (2.52) the quantum expression, the rate of probability can be expressed as (when $I_0 = \rho c$)

$$\frac{dP_{fi}}{dt} = \frac{\varepsilon(\tilde{\nu}) c \rho \ln 10}{N_a h\nu_{fi}} . \tag{2.53}$$

In order to obtain rate of probability of transition for the entire absorption band one has to integrate over the entire frequency range. Further by assuming ρ to be constant through out the band it results the following expression for the rate of transition probability dP_{fi}/dt

$$\frac{dP_{fi}}{dt} = \frac{c\rho \ln 10}{N_a h \nu_l} \int \frac{\varepsilon(\nu)}{\nu} d\nu = \frac{1}{6\varepsilon_0 \hbar^2} \left|\mu_{lm}\right|^2 \rho . \tag{2.54}$$

Rearranging the above equation the transitional dipole moment therefore expressed as follow

$$\left|\mu_{fi}\right|^2 = 3\frac{2\ln(10) c_0 \varepsilon_0}{N_a 2\pi^2} h \int \frac{\varepsilon(\tilde{\nu})}{\nu} d\tilde{\nu} . \tag{2.55}$$

The factor 3 in the above equation is due to the orientation averaging of the transitional dipole in isotropic medium.

The total intensity of the band obtained by measuring $\varepsilon(\tilde{\nu})$ in the regions of absorption and usually determine by integrating the area under the graph. So the integrated absorption coefficient due to transition [33] becomes

$$I_A = \int_{band} \frac{\varepsilon(\nu)}{\nu} d\nu = \int_{band} \frac{\varepsilon(\tilde{\nu})}{\tilde{\nu}} d\tilde{\nu} = \frac{1}{3} \frac{2h\pi^2 N_a}{\ln(10) c_0 \varepsilon_0} \left|\mu_{fi}\right|^2 = \frac{1}{3} S \left|\mu_{fi}\right|^2 \tag{2.56}$$

where

$$S = 2.9352 \times 10^{60} C^{-2} mole^{-1} .$$

2.4 Fluorescence Spectroscopy

Many chemical systems are photo-luminescent. That is they can be excited by electro-magnetic radiations and as a consequence, reemit radiation either of the same wavelength or of modified wavelength. The two common manifestations of photoluminescence are fluorescence and phosphorescence. With fluorescence, the luminescence ceases almost immediately after irradiation is discontinued, whereas phosphorescence usually endures for an easily detectable length of time [30].

According to Paulis's principle, the spins of the two electrons that occupy the same orbital must be anti-parallel. The total spin *S* of the molecule in the ground state is zero and the corresponding state of the energy of the molecule is termed "singlet state". After excitation, the electron spins may be either oriented parallel (triplet State, $S = 1$) or anti-parallel (singlet state, $S = 0$). The corresponding energies of these two possible states are different, because of the different interactions between electrons of parallel and anti-parallel spin. The energy of the triplet state is usually lower than the energy of the singlet state. Possible transitions are depicted in Jablonski diagram [30, 31].

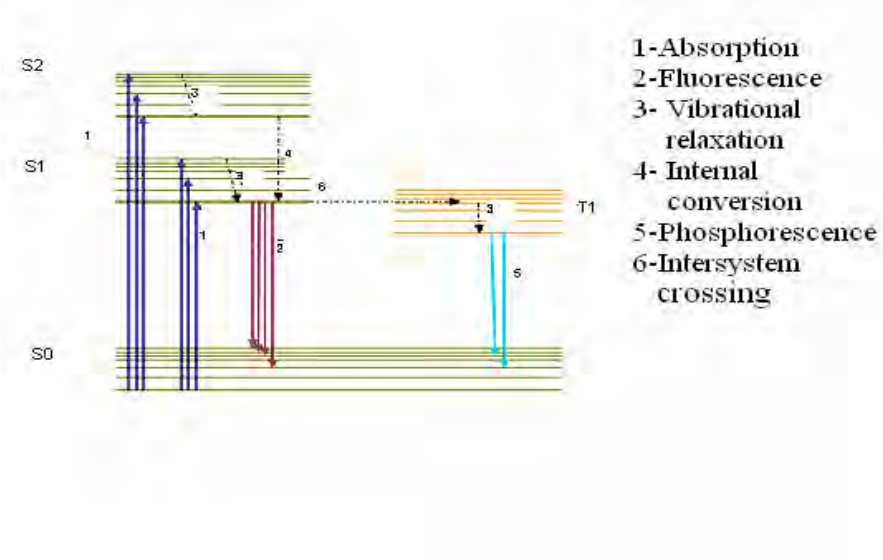

Fig 4: Jablonski diagram of transitions between different electronic energy levels.

2.5.1. Quantum Yield and Fluorescence Life Time

Both quantum yield and fluorescence lifetime are physical constants of the excited molecular species under a given condition of temperature and other environmental factors.

The contribution of fluorescence to the various deactivation processes of the excite state is termed the "quantum yield". The quantum yield Φ is defined by the quotient of the number of photons that are emitted and the number of photons that are absorbed [32].

$$\Phi = \frac{\text{number of emitted photons}}{\text{number of absorbed photons}} < 1 \qquad (2.57)$$

With the transition rates k_f for the fluorescence, k_Q for the different quenching processes, k_{ic} and k_{isc} for the internal conversion and for the intersystem crossing, and with the fluorescence quenching by quencher molecules, the quantum yield can be expressed as

$$\Phi = \frac{k_f}{k_f + k_{ic} + k_{isc} + k_Q} \qquad (2.58)$$

The higher the value of Quantum Yield the greater the fluorescence of the compound. A non-fluorescent molecule is one whose quantum efficiency is zero or close to zero. All energy absorbed by such molecules is rapidly lost by collision deactivation. There are many methods of determining Φ of substances. Using fluorescence standard substance is the most commonly used method [33, 36].

$$\frac{\Phi_1}{\Phi_2} = \frac{f_1 A_2}{f_2 A_1} \qquad (2.59)$$

where A is peak absorption and *f* is fluorescence integral area. The reciprocal of k_f is given by τ_f and is called the radiative lifetime of the lowest excited singlet state, or normally lifetime.

$$\tau_f^0 = 1/k_f \tag{2.60}$$

It is the mean lifetime of the excited molecule would spend in the excited state if fluorescence were the only means of deactivation of the excited state. Similarly

$$\tau_f = \frac{1}{k_f + k_{ic} + k_{isc} + k_Q}. \tag{2.61}$$

Is the lifetime of the lowest excited singlet state and corresponds to the actual mean time a molecule spends in the excited state.

2.5.2 Fluorescence quenching

The fluorescence of a substance is strongly affected by its environment. For example is the fluorescence quenching by so-called quencher molecules. These quencher molecules reduce the fluorescence quantum yield. The absorption process remains unaffected but the energy of the excited state is dissipated to the quencher molecules. There are two kinds of quenching processes that are dynamic quenching and static quenching. The efficiency of the two processes dependents the concentration of the quencher molecules [32, 36].

2.5.2.1 Dynamic Fluorescence Quenching

Considering fluorescence emission, internal conversion, and non-radiative transitions. The quantum yield in presence of fluorescence quenchers is given by Stern-Volmer equation.

$$I = I_0(Kc_Q\tau_0 + 1)^{-1} \tag{2.62}$$

where I is the intensity at a given concentration of quencher molecule c_Q, I_0 the initial intensity without the quencher, τ_0 the fluorescence lifetime and K is proportionality constant. The proportionality constant is termed quenching constant or Stern-Volmer constant.

2.5.2.2 Static Fluorescence Quenching

The fluorescence quenching by complex formation between the fluorophore M and the quencher molecule Q can be described by the following mechanism.

a)	$M + Q \rightarrow MQ$	Complex formation
b)	$M + h\nu_1 \rightarrow M^* \rightarrow M + h\nu_2$	Fluorescence
c)	$MQ + h\nu_2 \rightarrow (MQ^*) \rightarrow MQ + heat$	Quenching by the complex

If we assume that the quantum yield of the fluorescence in absence of quenchers is 1 ($\Phi_0 = [M^*]/[M] = 1$), then the quantum yield in presence of the quenchers may be given by

$$\Phi = \frac{\left[M^*\right]}{\left[M^*\right] + \left[MQ^*\right]}. \tag{2.63}$$

Combining the two equations results in

$$\frac{\Phi_0}{\Phi} = \frac{\left[M^*\right] + \left[MQ^*\right]}{\left[M^*\right]} = 1 + \frac{\left[MQ^*\right]}{\left[M^*\right]}. \tag{2.64}$$

If the probability of excitation is the same for the fluorescent molecule and the complex of the fluorescent molecule with the quencher, one can write

$$k_a[Q] = \frac{[MQ]}{[M]} = \frac{[MQ^*]}{[M^*]} \quad OR \quad k_a = \frac{[MQ]}{[Q][M]}. \tag{2.65}$$

The constant of complex formation k_a, therefore the ratio of the quantum yields can be expressed as

$$\frac{\Phi_0}{\Phi} = 1 + k_a[Q]. \tag{2.66}$$

If we replace the quantum yields with the corresponding intensities, we can get

$$\frac{I_0}{I} = 1 + k_a[Q]. \tag{2.67}$$

Static fluorescence quenching gives a linear dependence of the intensity ratio I_0 / I on the concentration of the quencher molecules. In contrast to static fluorescence quenching, the quenching of fluorescence by collision shows an additional dependence on the lifetime of the excited state of the fluorophore, which allows the distinction of two processes. This difference is immediately understood because the higher the probability of collision between the excited fluorophore and the quencher the higher the lifetime of the fluorophore. On the other hand, the formation of a complex will just reduce the concentration of the free fluorophore M and will not affect the lifetime of the excited molecules.

2.5.3 Concentration Dependence of Fluorescence

The intensity of fluorescence (emitted in all directions) is equal to the intensity of absorbed light multiplied by Φ. The fluorescence intensity I is the given as [32, 34, 36]

$$I = \Phi\left[I_0(1-10^{-\varepsilon cd}) \right] \tag{2.68}$$

where I_0 is the intensity of the exciting light (quanta per second), c is the concentration of the solution, d is the optical depth of the solution, ε is the molecular decadic absorption coefficient and Φ is the quantum efficiency. When the solution used is very diluted that the amount of light absorbed is very small, then the above equation may be reduced to

$$I = 2.3 \times I_0 \Phi \varepsilon cd \tag{2.69}$$

It is apparent that at such low concentrations when the exciting wavelength and intensity are kept constant, the fluorescence intensity will be directly proportional to the concentration of the fluorophore. Linear response will be obtained until the concentration of the fluorescent is sufficiently great so as to absorb less than 5% of the exciting radiation.

The fluorescence of concentrated solutions of fluorophores often shows a decrease in the fluorescence intensity, that is a decrease in quantum yield. This decrease is often coupled to changes in the spectral line shape and it has different reasons.

2.5.3.1 Reabsorption of Emitted Fluorescence Radiation

The higher the fluorescence, the higher the probability that another molecule reabsorbs the emitted radiation of a molecule. The condition for such reabsorption is that the emission and the absorption spectra partially overlap with each other. Reabsorption is therefore possible for the high frequency fraction of the emitted radiation.

The quantum yield for n reabsorption processes is dependent on the frequency, and the fluorescence emission disappears in the high frequency region. The shape of the fluorescence spectrum will change significantly, which can be reason for false interpretation of a fluorescence spectrum.

2.5.3.2 Dimer Formation

If dimers can be formed by monomers in the ground state the absorption spectrum will change since the dimers absorb radiation differently than monomers. The fluorescence spectrum of the monomer is often unaffected since the dimers are only rarely fluorescent. The appearance of dimers results in a reduced fluorescence intensity of the monomers.

2.5.3.3 Excited Dimers

Another concentration dependent mechanism that affects the fluorescence spectrum is the formation of excited dimers (excimers). Excited dimmers only exist in the exited state. The formation of excimers takes place only after excitation of one monomer that reacts with another monomer in the ground state. The absorption spectrum of the fluorophore remains unaffected by the formation of excited dimmers. However, in the fluorescence emission spectrum, an additional band appears (Figure 6). At low concentrations of the fluorophore excitation and fluorescence of the monomer are predominant. However, at higher concentrations the probability of excimer formation increases. The fluorescence of the excited D* appears at a different, usually lower frequency (higher wavelength).

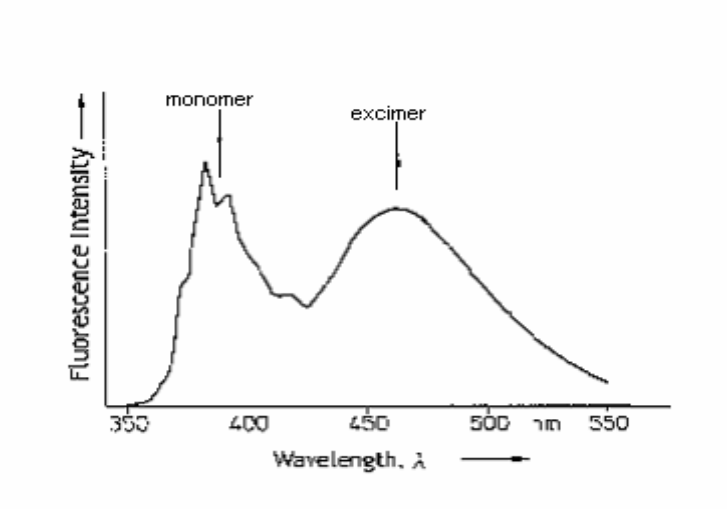

Fig 6: Fluorescence spectrum of Pyrene.

2.5.4 Temperature and Solvent Effects

The quantum efficiency of most molecules decreases with increasing temperature; because the increased frequency of collision at elevated temperature improves the probability deactivation by external conversion. Decrease in solvent viscosity also increases the likelihood of external conversion for the same reason, and leads to the same result [4, 32, 36].

Similarly to absorption spectroscopy, there are solvent effects on the spectral properties of fluorescent molecules. Changes in the fluorescence emission of a molecule can be caused by solvents of different polarity, of different dielectric constant or of different polarizability. In Figure 7, the appearance of possible red and blue shifts of the fluorescent light is explained by dipolar interactions of the fluorophore and the solvent. For reasons of simplicity, we assume that the molecule does not have a dipole moment in the ground state but only in the excited state. The length of the arrows that connect the two states gives the energy difference between the two electronic states.

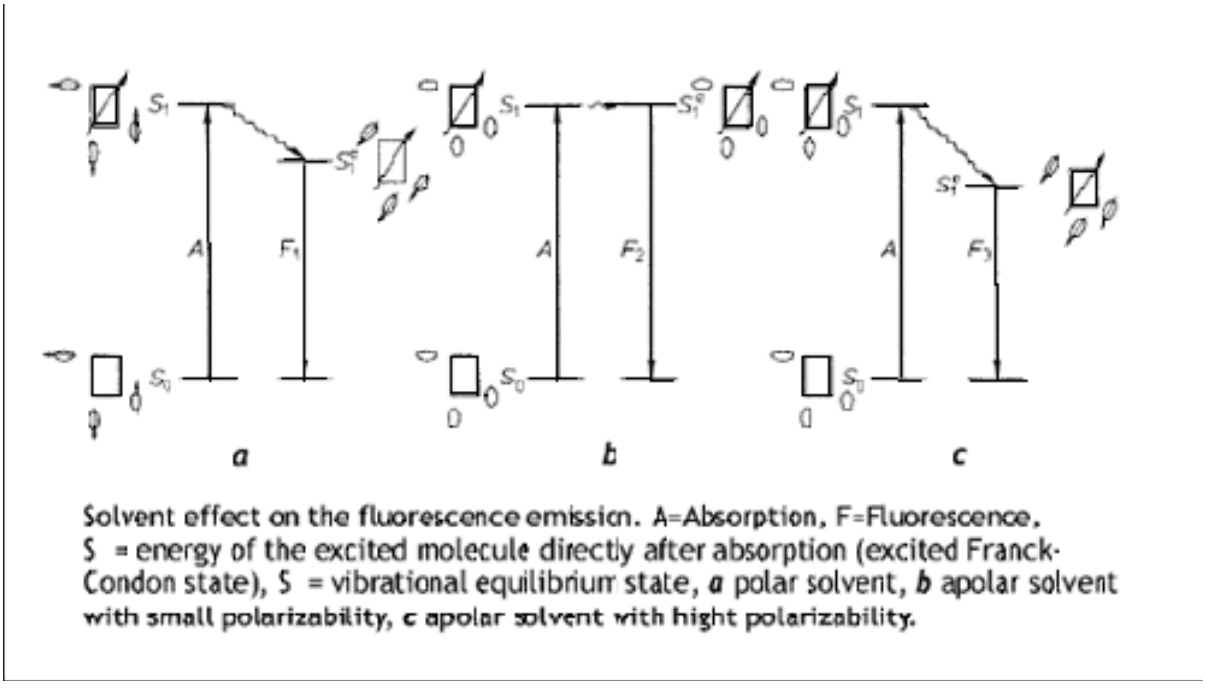

Solvent effect on the fluorescence emission. A=Absorption, F=Fluorescence, S = energy of the excited molecule directly after absorption (excited Franck-Condon state), S = vibrational equilibrium state, *a* polar solvent, *b* apolar solvent with small polarizability, c apolar solvent with hight polarizability.

Fig. 7: Red and blue shifts of the fluorescence of a molecule by different solvents.

First we shall consider the fluorescent molecule in a polar solvent. The excited Franck-Condon State S_1 has a higher energy than the equilibrium state of the excited molecule S_{1E}, which is reached after reorientation of the polar solvent molecules. If the molecule is in an apolar solvent (part b of Figure 7) there is no reorientation of the molecules in the apolar solvent, the energies of the states S_1 and S_{1E} (vibrational equilibrium state) are very similar to one another. The energy difference between the excited state from which the molecule fluoresces and the ground state is therefore bigger in a apolar solvent than it is in a polar solvent. Thus the emitted light is of higher frequency and smaller wavelength that is blue-shifted. If, in contrast, the polarizability of an apolar solvent is sufficiently high, than the excited fluorophore can induce dipole moments in the solvent and the energy of the equilibrium state of the fluorophore, S_{1E}, is reduced compared to the excited Franck-Condon state S_1. In this case, the energy level of the equilibrium state of the excited molecule in an apolar solvent of high polarizability is often lower than that in a polar solvent. The frequency of the emitted light is then smaller and its wavelength longer that is the fluorescence maximum of the emission spectrum is red-shifted. The solvent dependence emission spectra are interpreted interims of Lippert equation [36]

$$\bar{\nu}_A - \bar{\nu}_B = \frac{2}{hc} \times \left(\frac{\mu_e - \mu_g}{a^3} \right) \left(\frac{\varepsilon_r - 1}{2\varepsilon_r + 1} - \frac{n^2 - 1}{2n^2 + 1} \right) + cons\tan t \qquad (2.70)$$

where $\tilde{\nu}_A$ and $\tilde{\nu}_F$ are wave numbers of absorption and emission maxima respectively, h is plank's constant, c is speed of light, a is the radius of the cavity occupied by a single solute molecule. The first term to the left in the above equation is called orientation polarizability and is due to the reorientation of dipole and redistribution of electrons of the solvent molecules. Whereas the second term accounts for the redistribution of electrons.

The polarity of the solvent may also have an important influence energy of $\pi^* \leftarrow n$ transition is often increased in polar solvents, while $\pi^* \leftarrow \pi$ suffers the opposite effect in some instances such shift may be great enough to lower the energy of $\pi^* \leftarrow \pi$ process below $\pi^* \leftarrow n$ transition; enhanced fluorescence results.

Solvents containing heavy atoms or other solutes decrease fluorescence of compound. Orbital spin interaction in the solution also results in increase in the rate of triplet formation and a corresponding decrease in fluorescence. Fluorescence intensity is also sensitive to the pH of compounds.

2.5.5 Fluorescence and Structure

The most intense and useful fluorescence behavior is found in compounds containing aromatic functional groups with low energy $\pi^* \leftarrow \pi$ transition levels. Compounds containing aliphatic and alicyclic carbonyl structures or high conjugated double bond structures may also exhibit fluorescence, but it is small compared to aromatic systems.

Substitution of the carboxylic acid or carbonyl group on aromatic ring generally leads to an inhibition of fluorescence in these compounds the energy of the $n-\pi^*$ system is less than the $\pi-\pi^*$ system. The fluorescence yield of the former type of system is ordinary low.

It is found experimentally that fluorescence is particularly favored in molecules that posses rigid structures. Luck of rigidity in a molecule probably causes an enhanced internal conversion rate, and consequently increases for the likelihood for radiation less deactivation. One part of a non-rigid molecule can undergo low frequency vibrations with respect to its other parts; such motions undoubtedly accounts for energy loss [33, 37].

2.5.6 Derivative Fluorescence

We use fluorescence properties of substances for analytical and research purposes. The selectivity and sensitivity of spectrofluorometry made them preferable than the other spectroscopic methods. However, most substances are non-fluorescent or very weakly fluorescing, researchers use different methods to study such substances by modifying their absorption spectra [35, 37].

2.5.6.1 Metal Complexes

Complex of metals with organic and inorganic ligands, which absorb in the visible region of the spectra are of great importance in quantitative analysis. Transitions giving rise to colored complexes are of three types:

a) A $d-d$ transitions with in a transition metal ion: These are usually of low intensities and of little use for determination at trace levels.

b) Excitation with in an organic ligand: These are typical $\pi^* \leftarrow n$ and $\pi^* \leftarrow \pi$ transitions that are affected by the presence of a metal.

c) Charge transfer transitions: Involving the transfer of an electron between two orbitals one of which is associated predominantly with the ligand and other with the metal.

The last two types give rise to many strongly colored complexes suitable for trace analysis. Bands due to $d-d$ transitions are responsible for the colors of transition metal ions in aqueous solutions. Absorption of radiation results in the movement of electrons between filled and half field or empty metal d-orbital which differ in energy because of the electrostatic field created by coordination of the ligands. Various colors are produced depending on the metal and the nature of coordinating ligand. Absorption band shifted towards UV spectra with increasing strength of ligand field in the spectrochemical series. In most cases the bands are of low intensity because the transitions are spectroscopically forbidden by rules of symmetry. The fact that they occur at all is probably due to vibrational distortions that relax the rules. This does not apply to tetrahedral and square planar complexes which have no center of symmetry and which generally have quit intense absorption bands.

A large number of metal complexes involve organic ligands in which the absorption bands of the ligands are modified to a varying degree by coordination to the metals the effect on the spectra of the ligand depends on whether the metal-ligand bonds are predominantly covalent or ionic. In complexes where bonding to the metal is essentially ionic small shift in bands due to $\pi^* \leftarrow n$ and $\pi^* \leftarrow \pi$ transitions are absorbed with little change in intensity, the spectrum of the metal complex being smaller

to that of the protonated ligand. The stronger the complex formed, the more the absorption band is shifted towards the UV region.

Where the metal ligand bond is strongly covalent and possibly includes back bonding from metal to vacant ligand orbitals, the spectra of the ligand may be significantly changed. Complexes with metal forming more covalent bonds are shifted in to the near UV region because of modification of the conjugated ligands. The origin of charge transfer bands are quite different to those for the complexes already discussed associated mainly with covalent, and especially transition metal complexes, they are due to transition between σ or π ligand orbitals and empty or anti-bonding metal orbitals. Transition from σ metal orbitals to vacant ligand orbitals is also sometimes involved. These transitions are allowed by symmetry rules and consequently give much more intense bands than most $d-d$ transitions.

Chapter Three

3. Experimental Part

In this chapter basic instrumentation, materials and chemical used, sample preparation procedures and theoretical background used to analyze data are discussed.

3.1 Instruments

The instruments used in this work include Spectrofluorometer and UV/Vis Spectrophotometer. For all measurements quartz cuvette with 1 cm optical path length was used.

The instrument used for absorption measurement was UV/Vis/NIR Lambda 9 from PerkinElmer. The UV/Vis/NIR could operate in the spectral range from 190 nm to 2500 nm. The wavelength accuracy of the instrument is 0.2 nm. The manufacturer gives the photo-accuracy of 0.0001.

Spectrofluorometer from Shimadzu with model RF-5301PC was used for Recording emission spectra. The instrument operates from 220 nm to 900 nm. The light source used in the instrument is xenon lamp with the power output 150W.

3.2 Reflux

A liquid reaction mixture is placed in a vessel open only at the top. This vessel is connected to a condenser, such that any vapors given of are cooled back to liquid, and fall back into the reaction vessel. The vessel is then heated vigorously for the course of the reaction. The purpose is to thermally accelerate the complex formation by conducting it at elevated temperature. The advantage of this technique is that it can be left for a long period of time without the need to add more solvent or fear of the reaction vessel boiling dry as any vapor is immediately condensed in the condenser. In addition, as a given solvent will always boil at a certain temperature, one can be sure that the reaction will proceed at a constant temperature. By careful choice of solvent, one can control the

temperature within a very narrow range. The constant boiling action also serves to continuously mix the solution, although a magnetic stirring rod mechanism is often used to achieve a uniform solution. This technique is useful for performing chemical reactions under controlled conditions that require substantial time for completion.

3.3 Chemicals and Materials

Chemicals used for the experiment are: caffeine powder (Evan pharmaceutical company, England), $CuSO_4 \cdot 5H_2O$ (Aldrich, Germany), de-ionized water, Paraffin oil, bickers, stove, magnetic stirrer, (micro) pipettes, and electrical microbalance.

3.4 Experimental procedure

2 mg of caffeine and 0.2404 gm of CuSO4.5H2O are added to different bickers, which contain 200 ml of de-ionized water. UV/Vis spectra of these solutions were taken. 20 ml of caffeine solution was mixed and heated in a reflux with 20 ml of CuSO4.5H2O and then UV/Vis spectra of this solution were taken at t=0, 2, 4, 9, 11, 13, 15, and 17 hrs. And fluorescence emission of the complex is taken.

Chapter Four

4. Results and discussions

In this chapter all the results from the absorption and fluorescence emission measurements on caffeine and its complexes with Cu (II) are presented and discussed.

4.1 Absorption Properties of the Investigated Compounds and Complex

In order to investigate the formation of new derivative structures and also complexes the absorption spectra of the pure compounds of Caffeine, hexahydrated Copper sulphate, and their mixture and complex were recorded using UV/Vis spectrophotometer.

4.1.1 Absorption Spectra of Caffeine

The absorption spectrum of caffeine was measured in dichloromethane and water solution in the wavelength between 250 nm to 350 nm. From the spectra (Fig. 8) absorption maximum of caffeine was found at 272 nm and at 275 nm in dichloromethane and water solution respectively. The slight solvatochromic shift (3 nm) is an indication of an insignificant dependency of the electronic states through the reaction. Thus one can assign the absorption band to the $\pi^* \leftarrow \pi$. The moderate magnitude of the molar decadic absorption of caffeine at maximum absorption (ε_{max} =1045±13 m^2 mol^{-1}) further confirms the type of transition suggested.

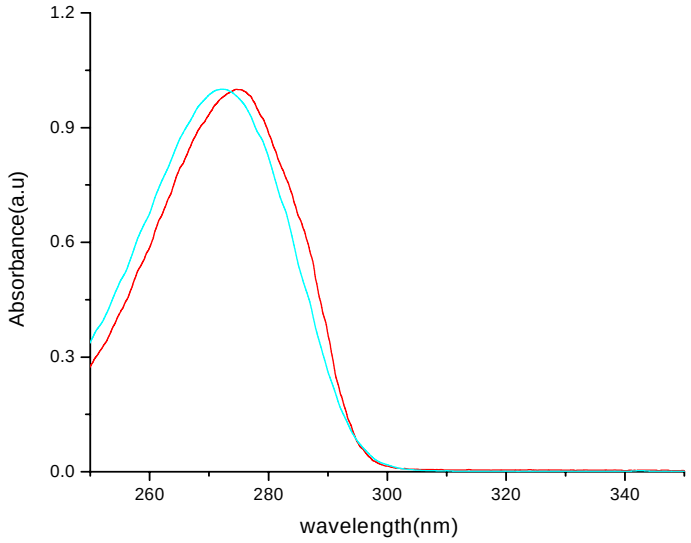

Fig. 8: Normalized absorption spectra of caffeine in dichloromethane (blue) and water (red) solution.

4.1.2 Absorption Spectra of $CuSO_4 \cdot 5H_2O$

$CuSO_4 \cdot 5H_2O$ was dissolved in water, and the absorption spectrum of the solution was recorded from 200 nm to 1100 nm. There was a strong absorption at around λ_{max} = 850 nm (Fig. 9). The intensity of the long wavelength absorption was very small compared to that of the short wave absorption. This indicates that the short wavelength absorption is due the allowed $\pi^* \leftarrow \pi$ in sulphate whereas the broadband transition centered at 850 nm is due to the forbidden $d-d$ transition in copper. Cu (II) has a d^9 configuration and thus the transition is between the electronic states $^2E_g \leftarrow ^2T_{2g}$, which is responsible for the deep blue color of the solution. Further it is observed that there is no absorption in the spectral range between 300 nm and 600 nm as can be seen from Fig. 9.

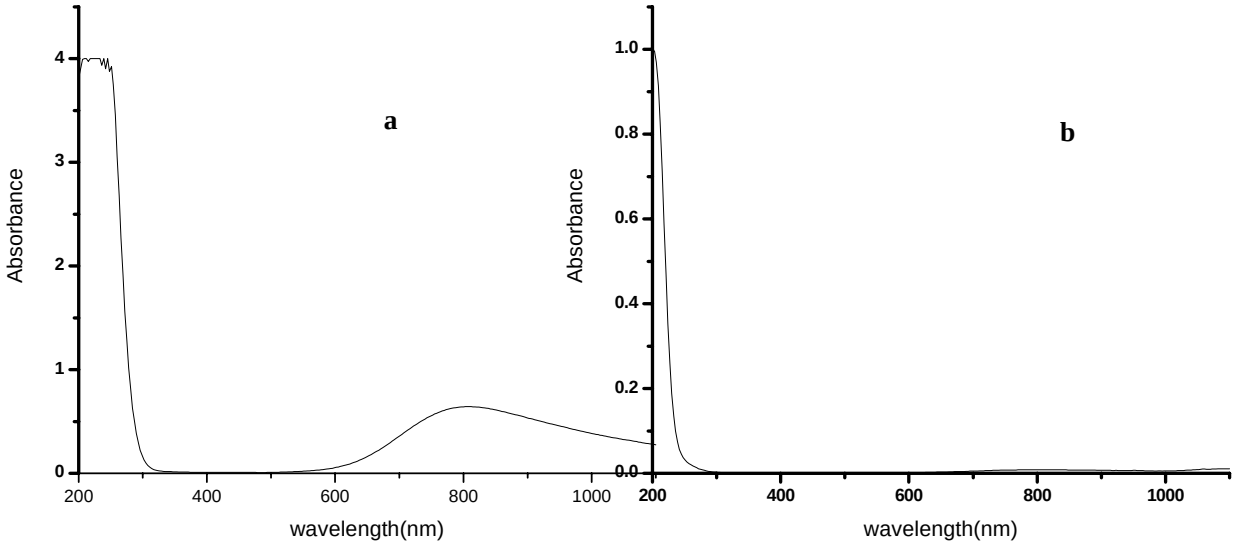

Fig. 9: Absorption spectrum of Cu (II) solution; a) concentrated and b) diluted.

4.1.3 Absorption Spectra of $CuSO_4 \cdot 5H_2O$-Caffeine Complex

$CuSO_4 \cdot 5H_2O$ and caffeine solutions were mixed in a given proportion and the absorption measurement was carried out after the solution was allowed to thoroughly mix for 30 minutes (Fig. 10). Two absorption peaks were found at 266 nm and at around 850 nm. Comparison of the spectrum of the mixture with that of the pure compounds enables one to assign the peak at 266 nm for $\pi^* \leftarrow \pi$ transition in caffeine and sulphate. And the other peak at 850 nm from Cu (II) $d-d$ transition. From Fig. 10 it is observed no absorption between 300 nm and 600 nm implying the formation of no new compound with different absorption properties with respect to the mixture constituting compounds.

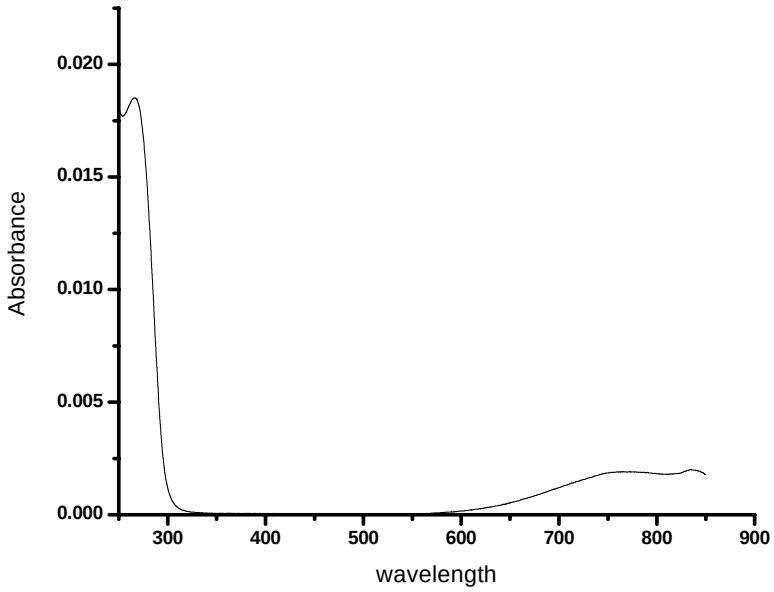

Fig. 10: Absorption spectrum of $CuSO_4$-caffeine mixture in water solution.

The mixture was then transferred to a refluxing apparatus. Sample spectra were taken in different time intervals and the refluxing continued until there was no significant change in the absorption spectra.

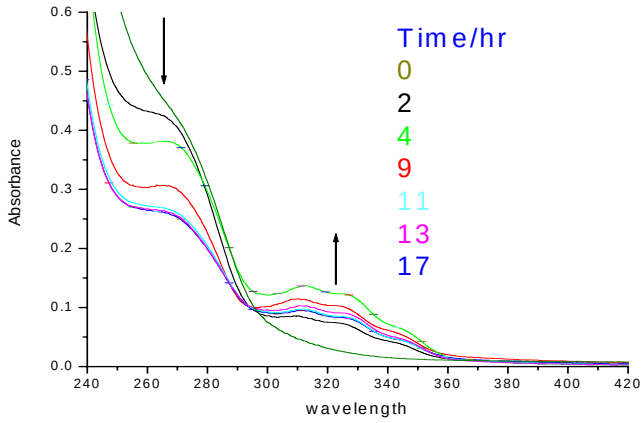

Fig. 11: Absorption spectra of Cu (II)-caffeine complex vs. wavelength.

Refluxing the mixture resulted in an appearance of multiple new bands between 300 nm and 360 nm with the position of the peak absorption at 313 nm as can be seen from Fig.11. The shoulders may have been resulted due to Frank-Condon vibrational progression or due to the convolution of different electronic transition. The absorbance of the bands (between 300 nm and 360 nm) increased as a function of refluxing time while the caffeine band peak absorption decreases as shown below in Fig. 12.

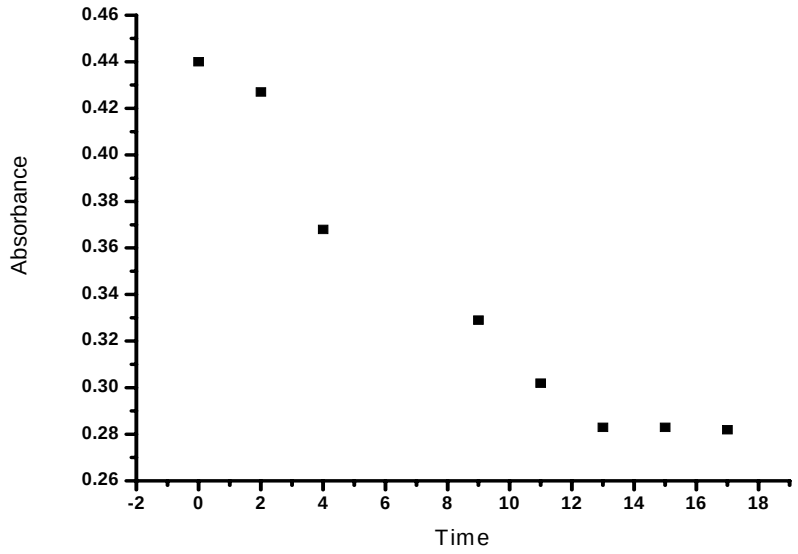

Fig. 12: Absorbance of caffeine vs. refluxing time @ 267 nm.

The decrease in absorbance of the caffeine peak is due to the decrease in concentration (Fig. 12), and the change in absorbance became small after 13 hr indicating the end of complex formation process.

4.2 Emission Properties of the Investigated Complex

Cu (II)-Caffeine complex which is heated in a reflux was investigated in a flourometry. Its fluorescence emission will be discussed in the following section.

4.2.1 Emission Spectra of $CuSO_4$ and $CuSO_4$-Caffeine Complex

The emission property of Cu (II)-caffeine complex, which was refluxed at about 11 hr was investigated. At the excitation wavelength λ_{exc} = 290 nm the emission spectrum (Fig. 13) showed very strong band with maximum intensity of emission at 411 nm. Comparison of emission intensities of the complex and the $CuSO_4$ suggests the large quantum efficiency of complex emission.

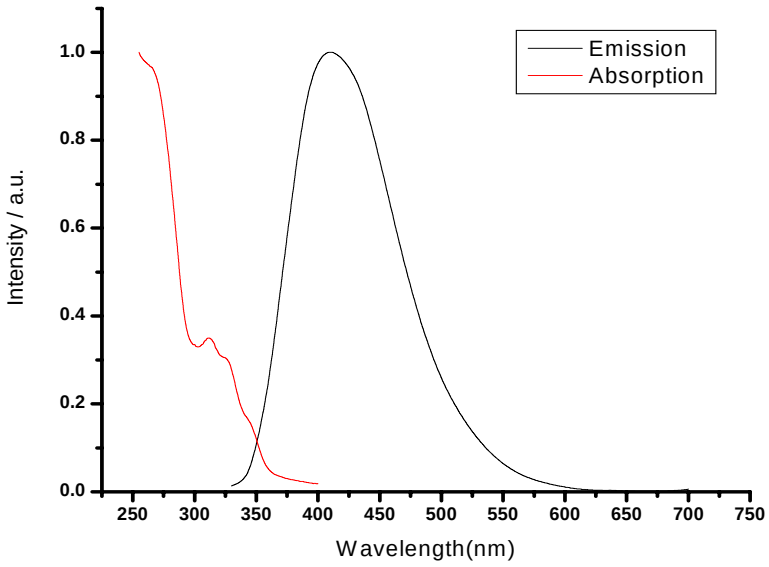

Fig. 13: Normalized Absorption and Emission Spectra of Cu (II)-Caffeine complex.

According to Kasha Rule for a single electronic transition the absorption and emission spectra should look mirror image to each other. However, from Fig. 13 it is evident that there are differences in the band shapes of absorption and emission. This suggests the existence of convoluted electronic transition bands in the ground and/or the excited states. In order to investigate these appearance excitation wavelength dependent emission measurements were undertaken and the results are shown in. The spectra are area normalized for the purpose of band shape analysis (Fig. 14).

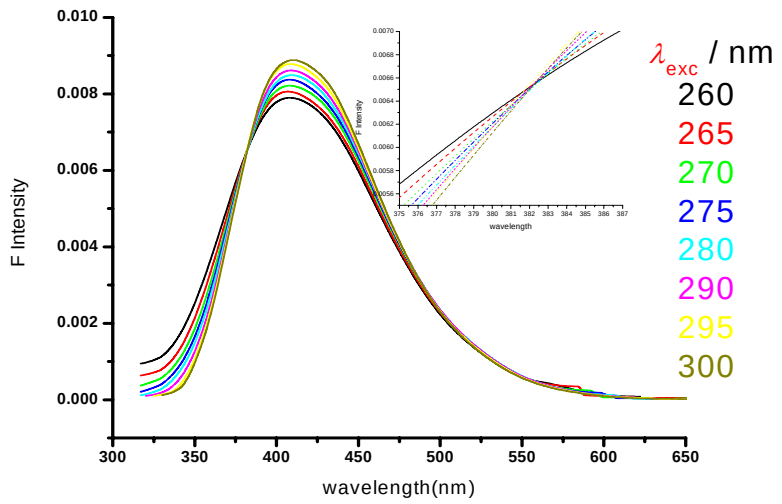

Fig. 14: Area normalized emission spectra of Cu (II)-caffeine complex at different excitation wavelengths. The embedded spectrum shows the iso-emission point.

The emission intensity at the emission maximum (@ 411 nm) increases successively as the excitation wavelength is increased from 260 nm to 300 nm, whereas; at the same time the emission intensities of the bands below 382 nm decrease. All the spectra have equal intensity at 382 nm. This wavelength is known as iso-emission point and is an indication of the existence of two systems or compounds in equilibrium. Since there are only Cu (II) and caffeine in the solution, the equilibrium system may be proposed to be composed of

$$\text{Cu(II)} + \text{Caffeine} \Leftrightarrow \text{Cu(II)} - \text{Caffeine Complex.}$$

Chapter Five

5. Conclusion

In this work the absorption and emission properties of pure caffeine, CuSO4, and mixtures and complexes of caffeine with CuSO4 were investigated. For caffeine wavelength of maximum absorbance λ_{max} was found at 272 nm and 275 nm in dichloromethane and water, respectively. Using Lambert-Beers Law for the molar decadic absorption coefficient ε_{max} a value 1045±13 m^2 mol^{-1} determined. Based on the moderate magnitude of ε_{max} and the insignificant solvatochromic shift the band is assigned to be $\pi^* \leftarrow \pi$.

$CuSO_4 \cdot 5H_2O$ shows a broad absorption band with $\lambda_{max} = 850\,\text{nm}$. This absorption bad centered at 850 nm is due to the forbidden $d-d$ transition in copper, and is responsible for the strong blue coloration of the compound in water solution. Cu (II) has a d^9 configuration and thus the transition is between the electronic states ${}^2E_g \leftarrow {}^2T_{2g}$.

In absorption study it was found that Cu (II) does not form complex with caffeine under room temperature. Refluxing Cu (II) caffeine mixture resulted in new absorption band where Cu (II) and caffeine do not absorb. This indicates the formation of complex, which is intensified with refluxing time. Equilibrium was reached after 11 hrs. The emission property of the complex was investigated. The emission was intense and thus fulfills the major criteria required for analytical application.

Caffeine is very weakly fluorescing compound. Quenching methods to determine caffeine content had been practiced [9, 10], but it was suffering because of the interference quenching by other molecules. Here fluorescence emission of Cu (II)-caffeine complex with relatively large quantum efficiency may be utilized for the determination of caffeine content in coffee in water solution. The possible selectivity of fluorescence compared to absorption may lead to selective determination not only to caffeine but also different compounds with extended π electron, especially herbicides.

Bibliography

1) P. B. Norton and J. Joseph, The new Encyclopedia Britannica, Encyclopedia Britannica Inc., Chicago, Vol. 3, 15th Ed., 1986, 1768.
2) A. Belay, Standard procedures to determine the percentage of caffeine in coffee seeds by UV/VIS spectrophotometer, A.A.U., MSc. Thesis, 2005.
3) F. L. Wellman, Coffee. Botany, Cultivation and Utilization, Leonard Hill, London, 2nd Ed., 1961, 56.
4) E. karatzis and T. papaioannou, Effects of solvent polarity and solvent polarity on the fluorescence properties of molecular rotors and related probes, J. bioorganic chemistry, Elsevier, 2005, 420.
5) E. Llly, The complexity of coffee, scientific American Inc., http://www.sciam.com/print_version.cfm?article ID=000E8EB9-949A-1CE5, 2002.
6) S. McCarthy, Ethiopia's coffee cooperatives: case study, presented to world bank, ACDI/VOCA, Washington DC, 2007, 8.
7) R. Goodacre and J. Gilbert, The detection of caffeine in a variety of beverages using curie-point pyrolysis mass spectrometry and genetic programming, J. Ins. of Biological science UK, The Analyst, 1999, 1074.
8) M. N. Clifford and K. C. Wilson, Coffee botany, biochemistry, and production of beans and beverages, Whitefriars press, London, 2nd ED, 1987, 45.
9) K. Ture, Optical qualitative and quantitative determination of caffeine in various coffee beans grown in Ethiopia, A.A.U., MSc. Thesis, 2005.
10) M. Memberu, Band deconvolution and fluorescence quenching methods for determination of caffeine in coffee seed, A.A.U., MSc. Thesis, 2006.
11) R. Coste, Coffee the plant and the product, MacMillan press, London, 1992, 5.
12) R. J. Clarke and R. Macrae, Coffee chemistry, Elsevier Ireland Ltd, Vol. 1, 1st ED, 2004, 425.
13) M. Nickels, M.D., Ph.D, Caffeine: is there grounds to concern?,

http://www.ittendojo.org/articles/health-2.htm - 10k, New York, 2001.

14) R.C. Baselt, Disposition of Toxic Drugs and Chemicals in Man, 7th Ed., Biomedical Publications, Foster City, CA, 2004, 157.

15) S. E. O'Connell and F.J. Zurzola, Rapid quantitative liquid Chromatographic determination of caffeine levels in plasma after oral dosing, J. Pharm. Sci.,1984, 1009.

16) A. A. Aldridge, J.V. Aranda and A. H. Neims, Caffeine metabolism in the newborn, J. Clin. Pharm., 1979, 447.

17) S. Bolton, and G. null, Caffeine psychological effects, use and abuse, orthomolecular psychiatry, Vol. 10, No. 3, 1981, 202.

18) D.Singh and A. Sahu, Spectrophotometric determination of caffeine and theophylline in pure alkaloids and its application in pharmaceutical formulations, J. Analytical Biochemistry India, Elsevier, 2006, 180.

19) P. Hewlett and A. Smith, Correlates of daily caffeine consumption, J. NCBI PubMed, Hospital and Community Psychiatry Denmark, Elsevier, Vol. 42 No 3, 2006, 97.

20) E. Karatzi, T. G. Papaioannou, and M. Myron, Acute effects of caffeine on blood pressure and wave reflection in healthy subjects, American Heart Association, Inc., 2001, 428.

21) A. Haarer, Arabian coffee planting and cultivation modern way, Mon. Bull, Indian coffee, Vol. 14, 1950, 7.

22) M. Sanchez, and J. Taillard, Sleep duration and caffeine consumption in French middle-aged working population, J. sleep medicine, department de Pharmacology France, Elsevier, 2004, 247.

23) S. Kerrigan and T. Lindsey, caffeine and fatal death: Two case reports, Am. J. epidemiology, 2005, 9987.

24) H. Ogita, H.Uefuji, Y.Yamaguchi, N.Koizumi and H. Sano, Diversity in bean Caffeine content among wild Coffee species, J. Food Chemistry, Vol. 91, 2004.

25) A. Ferreira, Caffeine as environmental indicator for assessing urban aquatic system, J. Artigo publica, 2005, 1889.

26) Y. Li Wei, C. Dong, S. Minshuang and Dian-Sheng Liu, Study for luminescence performance of three methyl Xanthene derivatives, J. ins. chemical engineering part A, 2005, 2585.

27) P. Atikins and R, S Friedman, Molecular quantum mechanics, Oxford University Press, 1st Ed., London, 1997.

28) P. Millonni, laser spectroscopy, John Wiley and Sons Inc., 4th Ed, New York, 1988, 120.

29) J. Jackson, Classical Electrodynamics, John Wiley and Sons Inc., 3rd Ed., New York, 1999, 47.

30) D. Skoog and D. M. West, Principles of instrumental analysis, Holt, Rine, Hart and Winstone Inc., 1st Ed., New York, Chicago, Sanfransisco, 1971, 27.

31) H. Bauer, G. D. Christian and J. E. O'Relly, Instrumental analysis, Harper & Row publisher, 2nd Ed., New York, 1978, 139.

32) A. Riddick, Fluorescence Assaying biology and Medicine, Elsevier, Sidney University, Sidney, 1962, 5.

33) G. M. Barrow, Introduction to molecular spectroscopy, McGraw-HILL, 1st Ed., New York, 1962, 25.

34) C. N. Raul, Ultra-Violet and visible Spectroscopy chemical applications, Whitefriars press, 3rd Ed., London, 1975, 128.

35) F.W. Fifield and D. Kealey, Principles and Practice of Analytical Chemistry, Blackie academic & professional, 4th Ed., London, 1995, 50.

36) B. Valeur, Molecular Fluorescence: Principles and Applications, Wiley-VCH Verlag GmbH, 1st Ed., London, 2001, 123.

37) W. B. Pearse, Identification of molecular spectra, Science press, Beijing, China, 1990, 145.